Responses to RC3:

General comments:

The authors derived the global balance wind (BU) in the height range of 18-100 km and latitudes of 50°S–50°N from 2002 to 2019 using the gradient wind approximation and SABER temperatures and modified by meteor radar observations at the equator. Using this data set, the authors examined the responses of zonal wind to QBO, ENSO and solar activity. MERRA2 zonal wind is used to validate BU and its response below 70 km. The manuscript is well organized and easy to follow. The interannual response as a function of month is an interesting result. My main concern is the dataset length and the significance test of the presented coefficients. BU has 18 years of data, to fit interannual response as a function of months, this means there are only 18 data points available for the fit. The manuscript did not present any significance test of fit. Rigorous significance test(s) should be added to make the results trustworthy to readers.

Response: Thanks for your careful reading and suggestions. Following your suggestion, the main improvement of this version can be ascribed to the following three points.

First, to elucidate the MLR model better and to remove the collinearity of predictors, the seasonal variations and the responses of winds to F10.7, QBO30 (QBOA), QBO10 (QBOB), and MEI are retrieved through three steps. Each step has specific purpose and formulae. We note that although the procedures of applying MLR is changed from that in the last version, this does not change the main results and conclusions significantly.

Second, we applied the same MLR procedure to the 40 years (1980–2019) of MERRA2 data (MerU40) and compared with the 18 years (2002–2019) of MERRA2 data (MerU18). Below ~55 km, the consistencies of the responses of MerU18 and MerU40 to QBOA and ENSO are better than those to F10.7 and the linear variations. Moreover, at ~40 km and above the equator, the significant negative linear variations of MerU40 coincide well with those MerU18.

Third, the statistical significance is estimated by p-value, which is used to replace the standard deviation in the last version.

Please see the point-to-point responses below.

More detailed comments:

1. More details should be added to explain the tidal aliasing at the equator. I assume tidal aliasing is not only an issue for 0 degree, it should be the equatorial region. How can a meteor radar station represent the zonal wind in the whole equatorial region? Is there any potential aliasing from semidiurnal tide in the mid latitudes?

Response: You are right, the tidal aliasing is not only an issue for 0 degree but also around the equatorial region. The detailed description on the balance wind (BU) data set can be found in Liu et al. (2021). Here, we provide a short description on the BU and also in the text (Sec. 2.1).

The gradient wind theory is formulated as,

$$\frac{\bar{u}^2}{a}\tan\varphi + f\bar{u} = -\frac{1}{a\bar{\rho}}\frac{\partial\bar{p}}{\partial\varphi} \tag{R1}$$

Equation (R1) is used to calculate the BU in the latitude ranges of 10°N–50°N and 10°S–50°S.

Above the equator, the BU is calculated as $\bar{u} = -(\partial^2\bar{p}/\partial\varphi^2)/(2\Omega a\bar{\rho})$ (Fleming et al. 1990; Swinbank & Ortland, 2003).

At 2.5°N–7.5°N and 2.5°S–7.5°S, the BU is estimated by a cubic spline interpolation of the BU at 10°N–50°N, 10°S–50°S and the reconstructed BU at the equator. This could remove the aliasing around the equator, at least to some extent.

How can a meteor radar station represent the zonal wind in the whole equatorial region?

Figure R1 shows the balance winds at the equator reported by Liu et al. (2021) and Smith et al. (2017). It can be seen the two datasets show a good consistency below ~80 km.
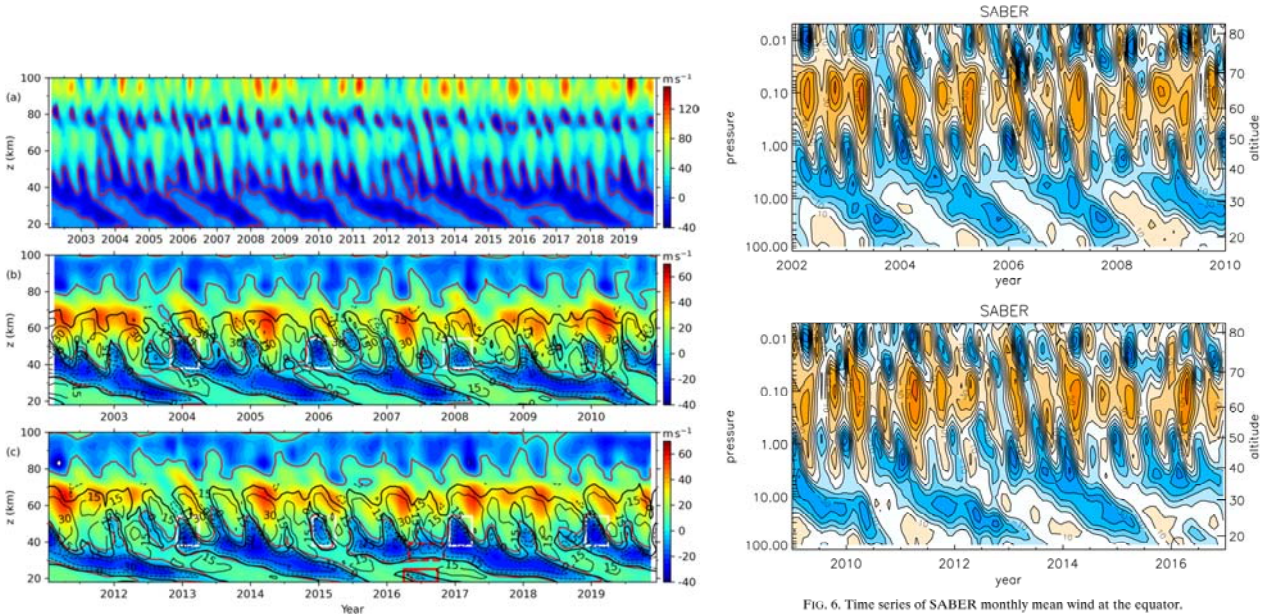
Figure R1: Balance winds at the equator reported by Liu et al. (2021, left column) and Smith et al. (2017, right column). The panel (a) of left column shows the theoretical balance winds from 18 to 100 km. The panels (b) and (c) the reconstructed balance wind, which is the wind in panel (a) replaced by the meteor radar observations at Koto Tabang (0.2ºS) above 80 km.

The monthly average of single point observation eliminates the aliasing from migrating tides and traveling planetary waves but contains the non-migrating tides and stationary planetary waves. For the consistency of balance wind and the monthly averaged zonal wind observed at a single station, Figure 3 of Smith et al. (2017) showed that the monthly zonal wind from a meteor radar at

Ascension Island (8ºS) coincides well with the balance wind at 81 and 84 km. This indicates that the monthly averaged zonal wind at a single station can represent the zonal average at least below 84 km. While above 84 km, the left column of Figure R1 shows that the theoretical balance winds are mainly eastward (upper panel (a) of the left column). In contrast, the reconstructed winds from a meteor radar observation at Koto Tabang (0.2ºS) are mainly westward. The differences between the theoretical balance wind and meteor radar observations are mainly the tidal aliasing above 84 km (Hitchman and Leovy, 1986; Smith et al., 2017; Xu et al., 2009). Moreover, the comparisons between the reconstructed balance winds with UARP (Atmosphere Research Satellite Reference Atmosphere Project wind climatology) and HWM14 (Horizontal Wind Model, Version 2014) exhibited general consistency above 80 km (Figures 6 and 7 of Liu et al., 2021).

Since the contaminations by non-migrating tides and stationary planetary waves cannot be excluded through monthly average at a single station in theory, further validation should be performed by comparing the monthly averaged winds at different longitudes but similar latitudes.
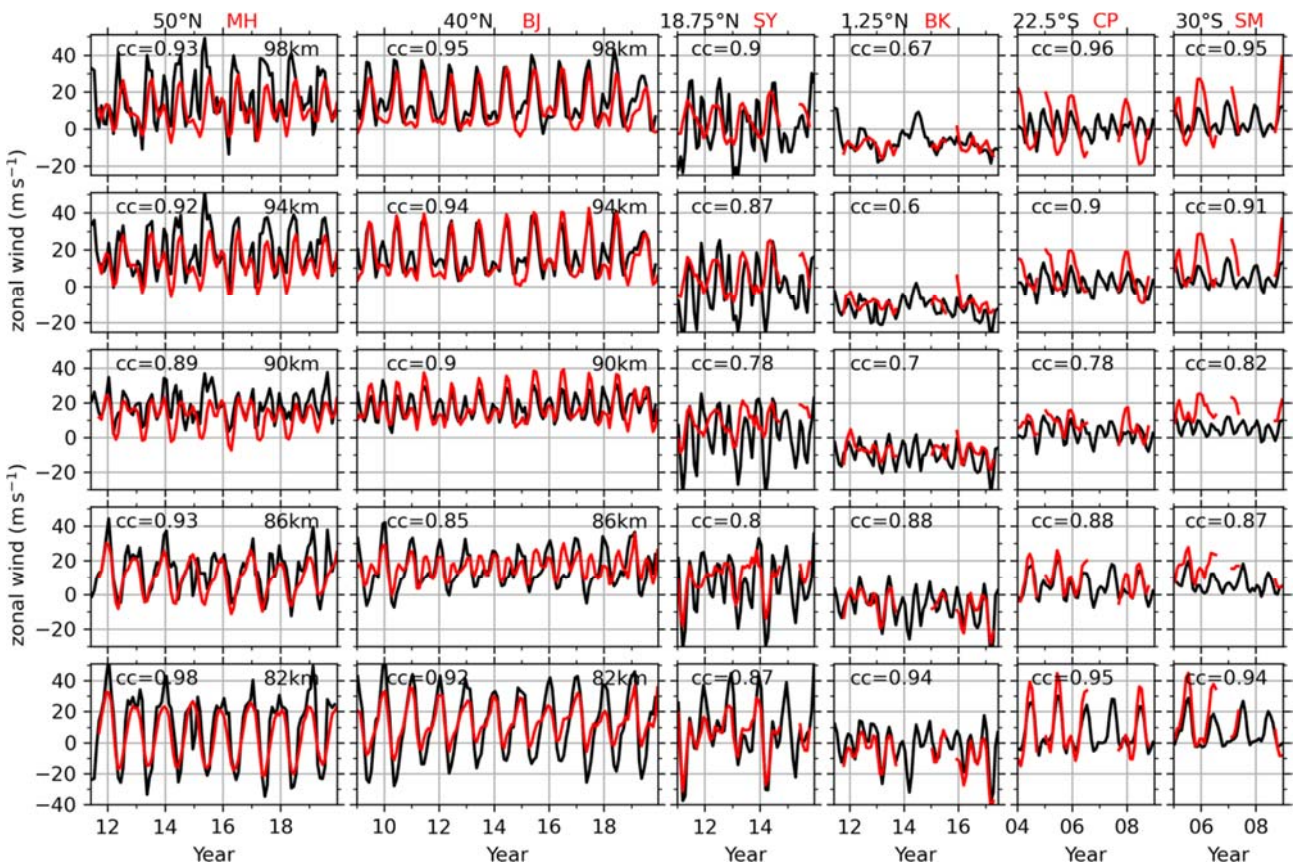
Figure R2: Monthly mean zonal wind from meteor radars (red lines, positive for eastward) at stations (from left to right) of MH (53.5°N), BJ (40.3°N), SY (18.3°N), BK (1.2°S), CP (22.7°S) and SM (29.7°S) and the BU (black) at the similar latitude (labeled on the top of each column) at five heights. The correlation coefficient (cc) between BU and MetU is labeled on each panel. Same y-axis is used in each row. The x-ticks mark the beginning of each year.

Is there any potential aliasing from semidiurnal tide in the mid latitudes?

Liu et al. (2021) compared the BU with meteor radar observations at six stations (Fig. R2). The comparisons among the time series of BU and meteor radar data illustrated that: At MH (53.5°N), BJ (40.3°N), BK (1.2°S) and SM (29.7°S) stations, the agreements between BU and MetU are good in general. The agreements are better at 82 km, 94 km and 98 km than those at 86 km and 90 km. At SY (18.3°N) station, the agreement between BU and MetU is good only at 82 km. At CP (22.7°S) station, the agreement between BU and MetU is good only below 90 km.

We think that the differences between BU and meteor radar data might be induced by the aliasing from semidiurnal tide in the mid latitudes. The first order approximation of momentum equation can be written as,

$$\frac{\bar{u}^2}{a}\tan\varphi + f\bar{u} + \frac{1}{a\bar{\rho}}\frac{\partial\bar{p}}{\partial\varphi} + \underbrace{\left(\frac{1}{a\cos\varphi}\frac{\partial\overline{v'v'}\cos\varphi}{\partial\varphi} + \frac{1}{\rho}\frac{\partial\rho\overline{v'w'}}{\partial z}\right)}_{gravity\ waves,tides,etc.} = 0 \tag{R2}$$

When we derive the balance wind, the contribution from waves (gravity waves, tides, etc.) are neglected (the term in the bracket of Eq. R2), which might cause aliasing to the zonal mean wind. Further study should be performed to assess the tidal aliasing on the zonal mean wind.

2. More details should be added to the MLR model especially on how the monthly coefficients for ENSO, QBO, and solar are obtained. How do you deal with the AO, SAO, and TAO when obtaining the monthly coefficients for interannual variability. Line 170, how does 42 parameters come about?

Response: This point should be clarified. In the last version, the regression model is,

$$u(t_i) = A_0 + \text{Season}(t_i) + \alpha F10.7(t_i) + \beta_{30}\text{QBO}_{30}(t_i)$$
$$+ \beta_{10}\text{QBO}_{10}(t_i) + \gamma\text{ENSO}(t_i) + \eta t_i + \text{Res}(t_i). \tag{R2}$$

Equation R2 is applied to data for 18 years. Moreover, the regression coefficients $\alpha, \beta_{30}, \beta_{10}, \gamma, \eta$ are not specific numbers but depend on the month. They have the form of (for example, α):

$$\alpha = \alpha_0 + \sum_{k=1}^{3}[\alpha_{2k-1}\cos(k\omega t_i) + \alpha_{2k}\sin(k\omega t_i)]. \tag{R3}$$

Here, $\omega = 2\pi/12$ (month). The regression coefficient of F10.7 in January is obtained by setting $t_i = 1$ in Eq. R3. In a same way, the regression coefficient in February can be obtained by setting $t_i = 2$ in Eq. R3, and so on. Then we can get the regression coefficients in 12 months. The annual mean regression coefficient is obtained by averaging the regression coefficients in 12 months. Moreover, Eq. R2 and (R3) play a role of de-seasonalizing regressor and predictors. This method was proposed by Randel and Cobb (1994) (Eq. 1 and 2 of their paper) and other researchers due to its highly compactable and portable in application.

In this version, to elucidate the MLR model better and to remove the collinearity of predictors, the seasonal variations, and the responses of winds to F10.7, QBO₃₀ (QBOA),

QBO$_{10}$ (QBOB), and MEI are retrieved through three steps. Each step has specific purpose and formulae. The detailed revision has been made in the text:

The detailed applications of MLR to retrieve the seasonal variations of winds and the responses of winds to F10.7, QBOA, QBOB, and MEI can be ascribed to the following three steps. For illustrative purpose, BU at 25°S and 50 km (black in Fig. R3a1) is taken as an example to show the procedure of MLR. This procedure is also applied to winds at other latitudes and heights, but results in different regressions coefficients due to the latitudinal and height dependencies of the seasonal variations and the responses of winds to F10.7, QBOA, QBOB, and MEI.
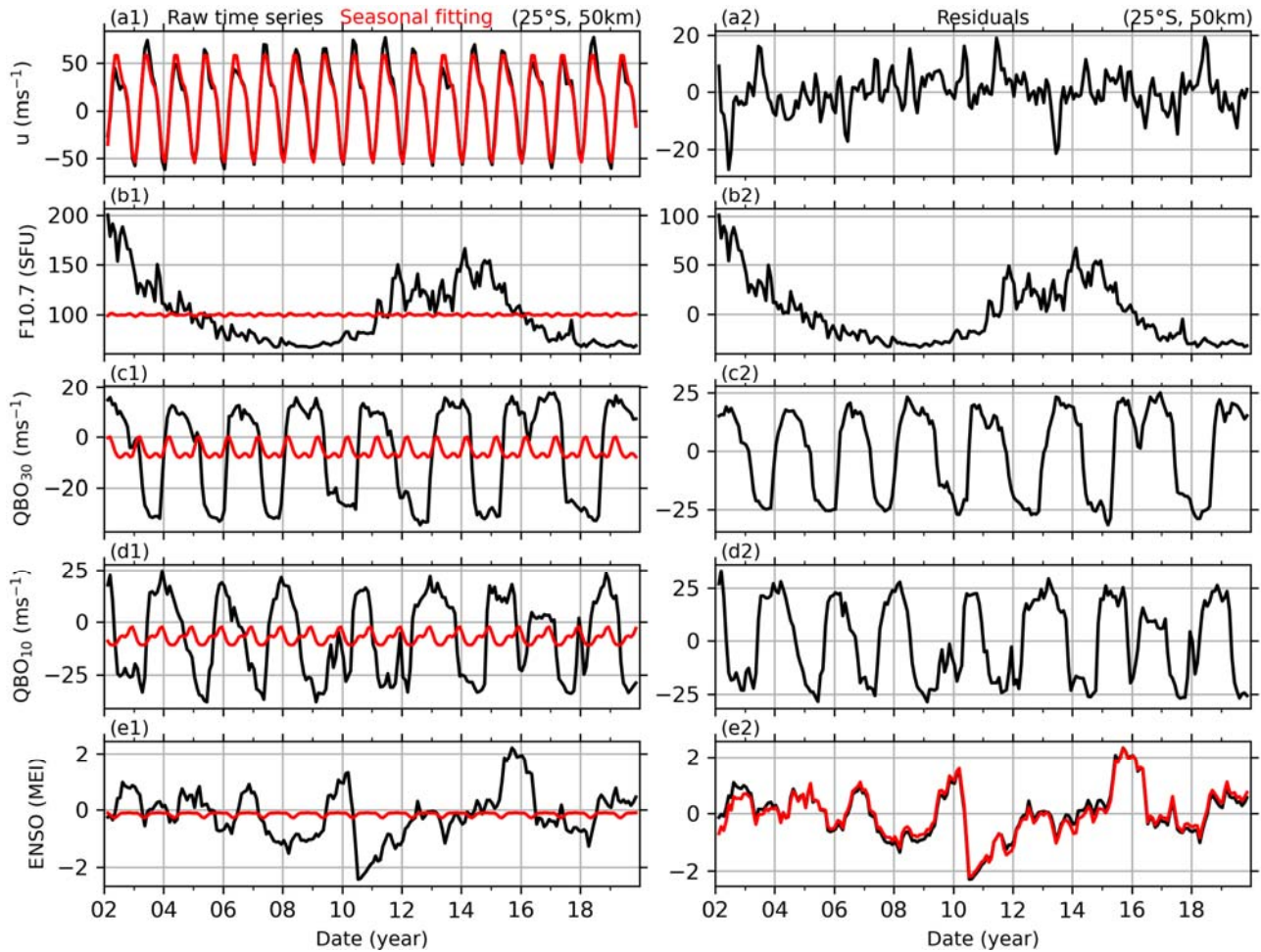
Figure R3: Example of the reference time series (left column) and their de-seasonalized results (right column). The first row: BU at 25°S and 50 km (black line in a1) and its seasonal fitting result (red line in a1), and the residual of BU (black line in a2). The second, third, and fourth rows: same captions as the first row but for solar activity (indicated by F10.7), QBO at 30 hPa (QBO$_{30}$ or QBOA) and at 10 hPa (QBO$_{10}$ or QBOB), and ENSO (indicated by MEI index). The red line in e2 is the residual of MEI index after removing the response of MEI to F10.7.

First, we de-seasonalize the wind and reference time series by fitting the following harmonics through the least squares method. At each latitude and height, the wind series is fitted as,

$$u(t_i) = u_0 + \sum_{k=1}^{3} A_k \cos[k\omega(t_i - \varphi_k)] + u_{res}(t_i). \qquad \text{(R4)}$$

Here, t_i $(i = 1, 2 \cdots, N)$ is the month number since February 2002. u_0 is the mean wind over the entire temporal interval, u_{res} is the de-seasonalized wind. $\omega = 2\pi/12$ (month), A_k and φ_k are the amplitude and phase of the annual (AO, $k = 1$), semiannual (SAO, $k = 2$), and terannual (TAO, $k = 3$) oscillations, respectively. In the same way, Eq. R3 is used to de-seasonalize the reference time series of F10.7, QBOA, QBOB, and MEI (shown in the left column of Fig. R3), and thus their residuals (F10.7$_{res}$, QBOA$_{res}$, QBOB$_{res}$, MEI$_{res}$, shown in the right column of Fig. R3) can be obtained and will be used as predictor variables (or explanation variables).

The rationality or goodness of the seasonal fitting result is quantified by R^2 score, which is the variations of the raw data explained by the model and defined as follows:

$$R^2 = 1 - \{\sum_{i=1}^{N} u_{res}^2(t_i)/\sum_{i=1}^{N}[u(t_i) - \bar{u}]^2\}, \quad \bar{u} = \frac{1}{N}\sum_{i=1}^{N} u(t_i). \qquad \text{(R5)}$$

The best fitting results in $R^2 = 1$, which means that the fitting result is the same as the raw data. For example, the seasonal fitting of BU at 25°S and 50 km is shown as red line in Fig. R3(a1). It coincides well with the raw BU series (black line in Fig. R3a1) with $R^2 = 0.967$. This means that Eq. R5 explains 96.7% of the variations of BU at 25°S and 50 km. Moreover, for this case, the fitting result shows that the AO has amplitude of 53.9 ms^{-1} and is in the dominant position. Then the SAO has a smaller amplitude of 13.2 ms^{-1}. While the TAO is the weakest and has amplitude of 3.9 ms^{-1}. The rationality of the fitting results (R^2) at other latitudes and heights will be shown in Sect. 3.1.

Table 1: The correlation coefficients and their p-values of regressors

	QBO30		QBO10		ENSO (MEI indx)	
	CC	p-value	CC	p-value	CC	p-value
F10.7	-0.0283	0.6803	0.0003	0.9965	0.2022	0.0030
QBO30			-0.0025	0.9705	0.0368	0.5921
QBO10					-0.0779	0.2567

Second, we check the multicollinearity among the predictor variables, which are the de-seasonalized F10.7, QBO30, QBO10, and MEI. The multicollinearity often leads to meaningless results if the correlation coefficients (CCs) between two or more predictor variables are significant. Here we calculate the CC and p-value of each pair of predictor variables (Table 1). If the p-value of a pair of predictor variables is less than 0.1 (or 0.05), one can state that the CC differs from zero at a confidence level 90% (or 95%). And thus, the multicollinearity of this pair is significant. In contrast, larger p-values indicate lower confidence level and insignificant multicollinearity. Table 1 shows that the CCs of most pairs are less than 0.1, and p-values are larger than 0.1. This indicates that the

multicollinearities of these pairs are insignificant and are approximately independent. On exception is the pair of F10.7 and ENSO, which has a CC of 0.2022 with p-value of 0.0030. This indicates that the multicollinearity of F10.7 and ENSO is significant at confidence level of 95%. To improve the independency between F10.7 and ENSO, a linear regression is performed with response variable of MEI index and predictor variable of F10.7. The residual of MEI index, which excludes the influences of F10.7, is used as a predictor variable to represent the effects of ENSO in the following MLR model. We note that the residual of MEI index is still noted as MEI_{res} in the following text. Now, the multicollinearity among the four predictor variables can be neglected and ensures a meaningful result of MLR in the next step.

Third, MLR is applied to get the responses of the de-seasonalized winds (i.e., u_{res} in Eq. R4) to the four predictor variables (F10.7$_{res}$, QBOA$_{res}$, QBOB$_{res}$, MEI$_{res}$) prepared in the second step. The MLR model is written as:

$$u_{res}(t_i) = \alpha \text{F10.7}_{res}(t_i) + \beta_A \text{QBOA}_{res}(t_i) + \beta_B \text{QBOB}_{res}(t_i) + \gamma \text{MEI}_{res}(t_i) + \eta t_i + \varepsilon(t_i) \quad \text{(R6)}$$

The regression coefficients $\alpha, \beta_A, \beta_B, \gamma$ indicate the responses of wind to F10.7, QBOA, QBOB, and MEI, respectively. The regression coefficient η is the linear variations or long-term trend. $\varepsilon(t_i)$ is the residual of the fitting and can be used to estimate the standard deviation and the p-value of each coefficient with the help of variance-covariance matrix and student-t test (Kutner et al., 2004; Mitchell et al., 2015). The monthly responses are obtained by selecting t_i in Eq. R6 only in that month of each of year. E.g., the response in January can be obtained by selecting the data only in January of each year. The annual responses are obtained by using all the data during 2002–2019.

3. Rigorous significance test should be added. I would suggest a Monte Carlo method. Other methods involve equations have underlying assumptions. If possible, multiple significance test methods should be used. 18 years data is short to study solar cycle, and 18 January is short to get interannual variability on the time scales of 2-5 years (ENSO and QBO) response on a monthly basis.

Response: Thanks for your suggestion, we have used the p-value to determine whether a regression coefficient is statistical significant in the new version.

The standard deviation is calculated by the variance-covariance matrix and the residuals of the MLR model (Chapter 6 of Kutner et al. (2004). For a MLR model of,

$$Y_{n \times 1} = X_{n \times p} B_{p \times 1} + \epsilon \qquad \text{(R7)}$$

Here $X_{n \times p}$ is the predictor matrix with p columns (the number of predictor variables) and n rows (observation times or sampling points). $Y_{n \times 1}$ is the response variable with observations times of n. $B_{p \times 1} = \{b_i : i = 0, 1, \cdots, p - 1\}$ is the expected regression coefficients of predictor variables. ϵ is a

vector of independent normal random variables. Due to the estimated $B_{p\times 1}$ by MLR model is unbiased, the variance-covariance matrix of $B_{p\times 1}$,

$$s^2\{B\}_{p\times p} = \begin{bmatrix} s^2\{b_0\} & s\{b_0,b_1\} & \cdots & s\{b_0,b_{p-1}\} \\ s\{b_1,b_0\} & s^2\{b_1\} & \cdots & s\{b_1,b_{p-1}\} \\ \vdots & \vdots & & \vdots \\ s\{b_{p-1},b_0\} & s\{b_{p-1},b_1\} & \cdots & s^2\{b_{p-1}\} \end{bmatrix} = \frac{\sum_{j=1}^n \epsilon_j^2}{n-p}\cdot(X'X)^{-1} \quad (R8)$$

The significance of the difference between b_i and 0 can be estimated by student-t test. For the confidence level of $1-\alpha$, student-t test states that,

$$\begin{cases} |b_j/s\{b_j\}| \le t(1-\alpha/2\,;n-p), & b_i = 0 \\ |b_j/s\{b_j\}| > t(1-\alpha/2\,;n-p), & b_i \ne 0 \end{cases}. \quad (R9)$$

Then the p-value is calculated from t-distribution table with $n-p$ degrees of freedom and α, that describes how likely to find a particular set of observations if the null hypothesis (i.e., the regression coefficient is 0) were true. The smaller the p-value, the more likely reject the null hypothesis and accept the no-null hypothesis (i.e., the regression coefficient is significant)
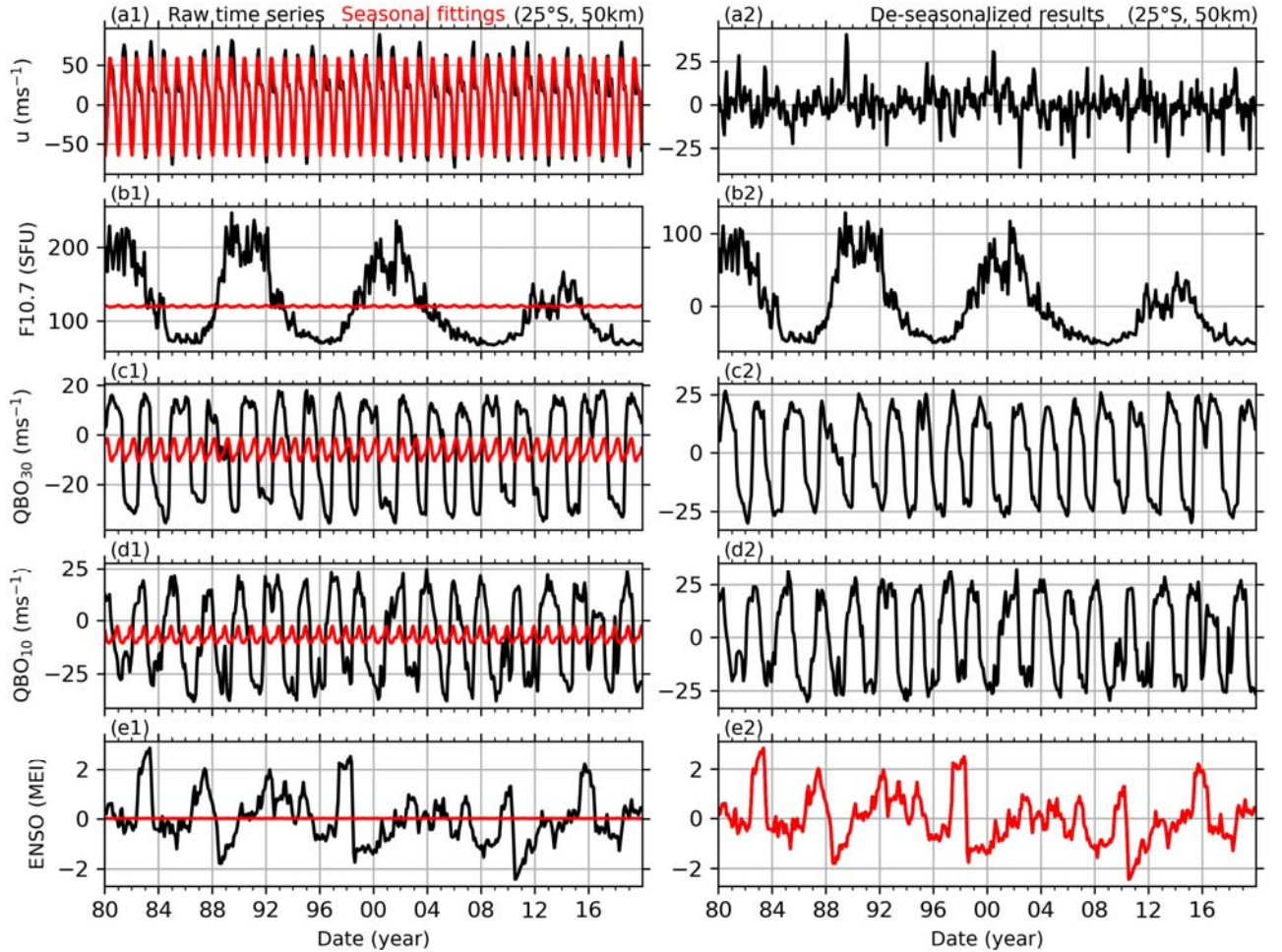
Figure R4: Example of de-seasonalizing MerU40 and the reference time series. The first row: BU at 25°S and 50 km (black line in a1) and its seasonal fitting result (red line in a1), and the residual of BU (black line in a2). The second, third, and fourth rows: same captions as the first row but for

solar activity (indicated by F10.7), QBO 30 hPa (QBO_{30} or QBOA) and 10 hPa (QBO_{10} or QBOB), and ENSO (indicated by MEI index). The red line in e2 is the residual of MEI index after removing the response of MEI to F10.7.

18 years data is short to study solar cycle, and 18 January months is short to get interannual variability on the time scales of 2-5 years (ENSO and QBO) response on a monthly basis.

To clarify this point, we performed the same procedure (see details in Respons#2 and in the text) on the 40 years (1980–2019) of MERRA2 data (MerU40). The monthly zonal mean wind at 25°S and 50 km is taken as an example to show the de-seasonalized results (Fig. R4) and MLR results (Fig. R5).
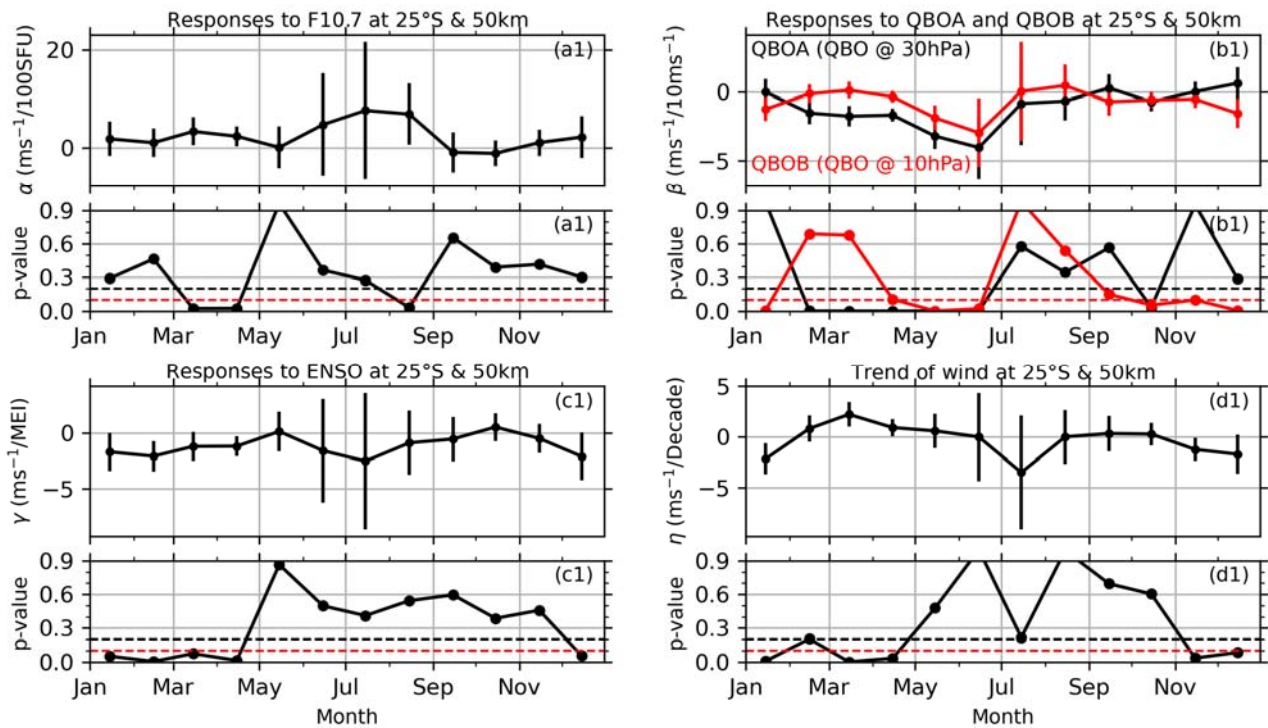
Figure R5: Example of retrieving the monthly responses of MerU40 at 25°S and 50 km (upper subplot of each panel) and their p-values (lower subplot of each panel) to solar activity (a1 and a2) QBOA (black in b1 and b2) and QBOB (red in b1 and b2), ENSO (c1 and c2), and the linear variations (d1 and d2). The error bars are the confidence interval at 90% confidence level.

Figure R4 shows that the seasonal variations are important in the wind (Fig. R4a1 and a2) but are insignificant in the time series of F10.7, QBO_{30} (QBOA) , QBO_{10} (QBOB), and ENSO (Fig. R4b1-e2). Figure R5a1 shows that the responses of MerU40 to F10.7 are significant (p-value ≤ 0.1) in March, April, and August. This is different from the responses of the 18-year data (short for MerU18) to F10.7, which are significant only in May. The responses of MerU40 to QBOA and

QBOB (Fig. R5b1) are significant in April–June and in October. This is similar to those of MerU18, which are also significant in May–June, but insignificant in April and October. The responses of MerU40 to ENSO (Fig. R5c1) are negative and significant in January–April and December. However, the responses of MerU18 to ENSO are also negative but are insignificant. The linear variations of MerU40 (Fig. R5d1) are significant in March and April (positive values) and in November and December (negative values). However, the responses of MerU18 are insignificant (judged by p-value > 0.1) in all months.
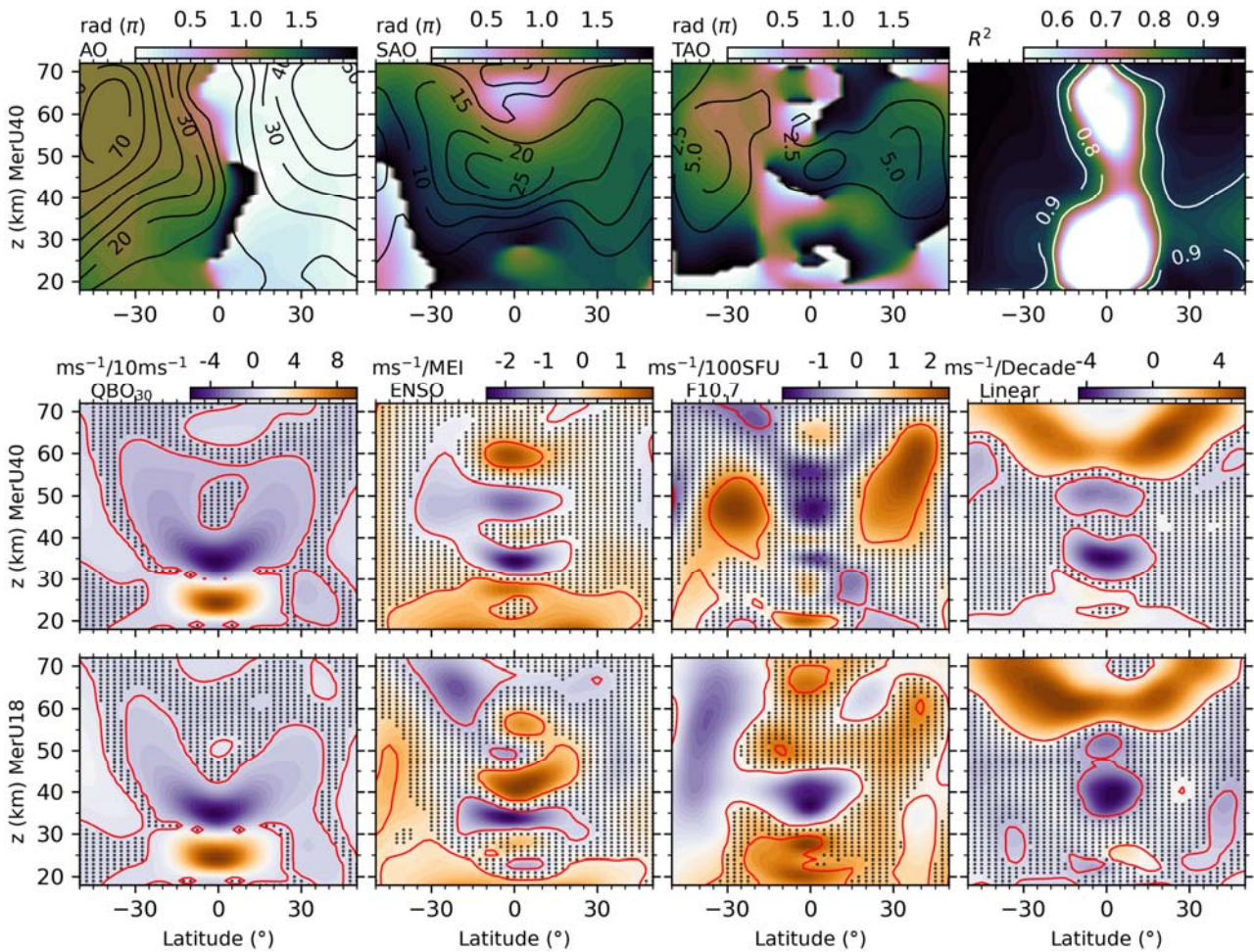
Figure R6: Upper row: the latitude-height distributions of the amplitudes (contour lines) and phases (color scale) of seasonal variations and the R^2 scores (from left to right) of MerU40. Middle row: the latitude-height distributions of the responses of MerU40 to QBOA, ENSO, F10.7 and linear variations (from left to right). Lower row: same caption as the middle row but for the MerU18. The black dots indicate that the regression coefficients with p-values larger than 0.2. The red lines indicate the regression coefficients with p-values of 0.1.

Figure R6 shows the seasonal variations of MerU40 (upper row) and the responses of MerU40 (middle row) and MerU18 (lower row) to various predictors. We see that AO, SAO, and TAO of MerU40 exhibit similar latitude-height distributions as those of the MerU18. The responses of

MerU40 to QBOA are similar to those of MerU18 on the aspects of magnitudes and patterns but have a wider significant region around the equator. Around the equatorial region, the responses of MerU40 to ENSO have similar patterns to those of MerU18 around the equatorial region. However, the positive responses of MerU40 to ENSO are stronger (weaker) than those of MerU18 below ~30 km (around ~40–45 km). Around ~20°S and above ~55 km, the negative responses of MerU18 to ENSO are stronger than those of MerU40. At ~40°S and around ~30 km, the significant positive responses of MerU18 to ENSO cannot be seen in those of MerU40. The significant responses of MerU18 to F10.7 occur in wider height ranges as compared to those of MerU40 around the equator. Moreover, at latitudes higher than 30°S, the responses of MerU18 to F10.7 are negative as compared to the positive responses of MerU40 to F10.7. At around 40°N and ~40–60 km, the positive responses of MerU18 to F10.7 are weaker and less significant than those of MerU40. The linear variations of MerU18 coincide with those of MerU40 above ~30 km, except around ~45°N/S, where the negative linear variations of MerU40 (MerU18) are significant (insignificant). Below ~30 km, the positive linear variations of MerU40 extend to wider latitudes as compared to those of MerU18.

A summary of the responses and linear variations of MerU18 and MerU40 below ~55 km (this is most reliable height since the damping is significant above this height (Ern et al., 2021)) is below. **The consistencies of the responses of MerU18 and MerU40 to QBOA and ENSO are better than those to F10.7 and the linear variations. Moreover, at ~40 km and around the equator, the significant negative linear variations of MerU40 coincide well with those MerU18.**

4. Figure 1 g, the R^2 value is 0.98. This number is somewhat misleading since I assume the goodness of fit is mainly coming from seasonal fit. How good is the fit if only interannual variability is considered?

Response: Comparing the $R^2 = 0.967$ of this version and the $R^2 = 0.98$ of the last version, we see that the goodness of fit is mainly coming from seasonal fit. This confirmed you assumption. This also illustrate that the monthly zonal mean wind (at least for the wind at 25°S and 50 km), the seasonal variations are in the dominant position as compared to the contributions from predictors (F10.7, QBOA, QBOB, ENSO, and linear variations).

The goodness of the fit if only interannual variability is considered can be assessed through ε in Eq. R6 and then the student-t in Eq. R9. If the fitting result is good, this will induce small ε and small variance $s^2\{b_j\}$ in Eq. R8, and then the ratio $\left|b_j/s\{b_j\}\right|$ in Eq. R9 should be large. This will provide large probability of accepting $b_i \neq 0$ and high confidence level (small p-value) of estimating b_i. Thus, the p-values shown in Fig. R5 in Responses#3 and Fig. 2 in the text provide an assessment of the goodness of fitting. However, the p-values in Fig. R5 and Fig. 2 are less than 0.1

(confidence level of 90%) only in some limited months. This indicate that the goodness of fitting the interannual variabilities are not as good as that the seasonal fitting results.

Moreover, Fig. 3–7 in the text show that the regions with p-values ≤ 0.1 (confidence level of 90%) occurs only in a limited latitude and height ranges. Thus, the goodness of fitting the interannual variabilities are not as good as that the seasonal fitting results in most latitudes and heights. This might be caused by the dynamic process such as wave-mean flow interaction and the non-uniform distribution of wave sources in the atmosphere, and by the chemical process such as ozone heating in the stratosphere and CO_2 cooling in the mesosphere.

It should be noted that the regions with p-values ≤ 0.1 indicate the responses of the monthly zonal mean wind to predictors are significant.

5.   In the discussion of the effects of the data interval, I share another reviewer's point of view: all the data intervals are overlapped somewhat. At least two totally separate data intervals should be used. Significance tests should be added here as well.

Response: I agree with your idea that at least two totally separate data intervals should be used. However, if we separate the 18 years (2002–2019) (MerU18) into two totally separate data intervals, each interval is approximately 9 years, which cannot cover one solar cycle.

To clarify this point, we performed the same procedure on the 40 years (1980–2019) of MERRA2 data (MerU40) (See Responses#3 for detail). Comparing between the results from MerU40 and MerU18, we see that below ~55 km (this is most reliable height since the damping is significant above this height (Ern et al., 2021)), the consistencies of the responses of MerU18 and MerU40 to QBOA and ENSO are better than those to F10.7 and the linear variations. Moreover, at ~40 km and around the equator, the significant negative linear variations of MerU40 coincide well with those MerU18.

Significant tests have been performed through student-t test and p-value.